Effect of injector nozzle flow number on injection evolution in a transparent diesel engine operating with pure RME fuel

E. Mancaruso[1*], B. M. Vaglieco
Istituto Motori - CNR, Italy
e.mancaruso@im.cnr.it and b.m.vaglieco@im.cnr.it

Abstract

The present paper describes an experimental investigation over the impact of diesel injector nozzle flow number on both injection and combustion evolution in transparent compression ignition engine equipped with modern Euro5 light-duty diesel engine head and the production common rail injection system. The research activity is devoted to understanding the basic operating behavior of low flow number nozzles, which are showing promising improvements in diesel engine behavior at partial load. In fact, because of the compelling need to push further emission, efficiency, combustion noise and power density capabilities of the last-generation diesel engines, the combination of high injection pressure fuel pumps and low flow number nozzles is popular among major OEMs.

Therefore, aim of this paper is to provide a deeper understanding about the link between the nozzle flow number, the spray and mixture formation and the consequent combustion behavior for nozzle geometries and engine operating conditions that are typical of last-generation diesel engines operating with pure RME fuel. This will generate guidelines for the balanced nozzle flow number selection based on engine targets as well as will generate reference spray for upgrading 3D-CFD simulations models.

Spray opening angle, break-up length and tip penetration are evaluated for three different nozzle flow numbers for a 2.0L diesel engine in various operating conditions. The results confirm that by reducing the flow number, for low injected quantities typical of low load and speed engine operating conditions, better fuel/air mixing improves the emissions/fuel economy trade-off.

Introduction

The combustion process is highly dependent on the fuel injection parameters. Therefore, precise control over fuel injection, and thus the spray formation, is essential in controlling the combustion process. In particular, in order to further increase the performance and emission characteristics of compression ignition engines it's very important to study fuel atomization and spray processes which in turn are strongly influenced by the flow dynamics inside the injector nozzle [1, 2]. Understanding of the maximal penetration of liquid fuel into the cylinder is crucial to avoid wall-wetting, which can lead to unacceptable emission levels, especially with early injection strategies. The liquid length is also important to understand the general behavior of a combustion fuel spray. Since several regimes can occur, it is crucial to measure, analyze and understand liquid length and fuel distribution into the engine.

On the other hand, the possibility to analyze the injection process directly into the engine and under the same real engine operating conditions can help to understand in better way the fuel atomization and evaporation with respect to the analysis in more simple system like the controlled temperature and pressure vessel or the rapid compression machine. The opportunity to use an optical engine equipped with the real engine head and the last generation common rail injection guarantees that the intake air motions and the fuel/air interactions are preserved. Moreover, when the engine running in continuous mode, the effect of the heat exchange between the hot surfaces of the engine, the combustion zones, and the spray, on the penetration, fuel dispersion and evaporation, respectively, must be considered too.

This paper deals with a study that involves the fuel injection in a single-cylinder engine in order to assess the biodiesel and nozzles types on mixture behavior. The multi injection strategy has been performed with last generation Common Rail (CR) high pressure injection system. It is typical of new generation Euro 5 diesel engine and consists of two injections per cycle. Transparent DI diesel engine with the head of 2.0 L, Euro5, production engine has been used. The investigation has been performed with three 8-hole nozzles with different flow number fuelled with both diesel fuel as reference (REF) and pure Rapeseed Methyl Ester (RME) as biofuel.

* Corresponding author: Ezio Mancaruso, Istituto Motori-CNR, Via G. Marconi, 8 – 80125 Napoli
Tel-fax: +390817177187 - +390812396097 – email: e.mancaruso@im.cnr.it

Experimental Methods

The study of the spatial and temporal evolution of the fuel jets has been carried out in an optically accessible diesel engine. It is a single-cylinder engine equipped with cylinder head and common rail injection system derived from a four-cylinder, 16 valves, 2.0 liter, Euro 5 production engine (Figure 1).

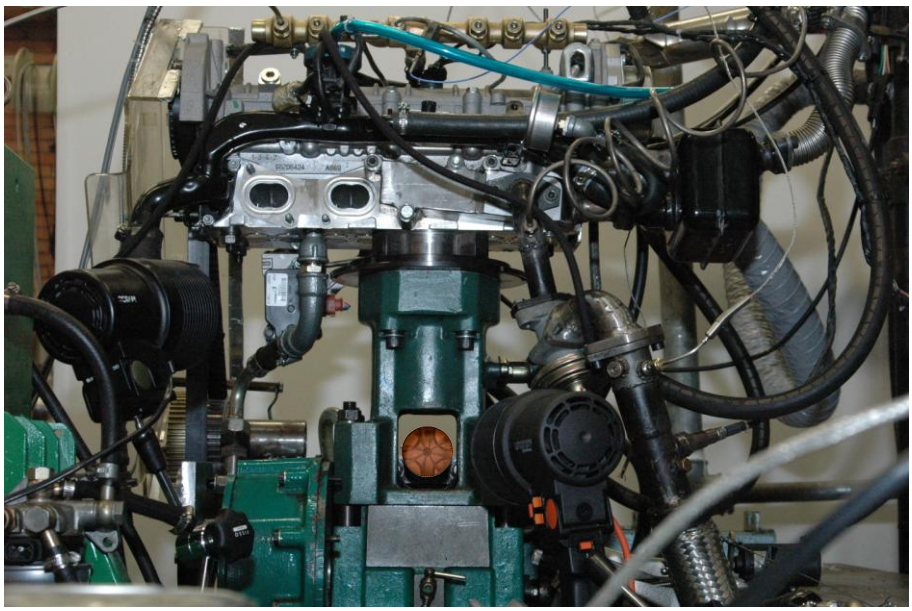

Figure 1: Transparent engine

The engine stroke and bore are 92 mm and 85 mm, respectively; and the compression ratio is 16.5:1. An external air compressor has been used to supply pressurized intake air in order to obtain the same in-cylinder conditions of the real multi-cylinder engine and to compensate lower compression ratio, typical of the optical engines. Moreover, the intake air, before reaching the intake manifold, is filtered, dehumidified, and preheated. A variable swirl actuator (VSA) system has been employed in order to manage the air swirl motion in the intake manifold. In the exhaust pipe, the presence of a pressure valves permits the recirculation of the right amount of burned gases through the cooled Exhaust Gas Recirculation system (EGR). Finally, the engine has been equipped with a second-generation CR system. The injector has been controlled by a fully flexible Electronic Control Unit (ECU) for combustion optimization. In order to provide a full view of the combustion bowl a 46 mm diameter flat window has been fitted in the piston head and an appropriate 45° visible fixed mirror has been set inside the extended piston. The window has been realized with UV-grade fused silica. In order to analyze the injection signals, a Hall-effect sensor has been applied to the line of the solenoid current. Moreover, to acquire the in-cylinder pressure in motored and fired condition, a piezoelectric pressure transducer has been set in the glow plug seat of the engine head. For each operating condition investigated, the cylinder pressure and the drive injector current have been digitalized and recorded at 0.1 crank angle degree (°CA) increments and ensemble-averaged over 150 consecutive combustion cycles. At motored condition, temperature and density at Top Death Centre (TDC) were estimated, assuming a polytropic coefficient of 1.36 [3]. Considering that the intake air temperature and pressure were set to 317 K and 1.1 bar, respectively; the in-cylinder temperature and density average for the three nozzles were 818 K and 18.7 kg/m^3, respectively.

Digital imaging analysis has been performed by a CCD camera. The CCD camera (640 x 480 pixels) had a high sensitivity over a wide visible range and it has been equipped with a 55 mm objective F/1:3.5 and another Macro objective 90 mm focus length and F/2.8. Images have been acquired with an exposure time of 0.055 ms corresponding to 0.5°CA at 1500 rpm. Two external highly luminous CW halogen lamps have been used to light the combustion chamber during the injection process. More details of the engine and the experimental set up are reported in previous paper [4].

The engine operating condition has been extracted from the ECU map of a commercial Euro5 engine; it represents the condition at 1500 rpm at 2 bar of brake mean effective pressure (BMEP). The implemented injection strategy consisted of pilot + main pulses and has been fixed for all the flow numbers and fuels tested. In particular, three injectors equipped with 8-holes nozzle, minisac-type, and different flow numbers have been adopted. Hereafter, they will be labelled as A for 0.136 mm in diameter, B for 0.122 and C for 0.107 mm producing 480, 390 and 300 cc/30 s @100 bar, respectively. In Table 1, the engine operating conditions are reported Moreover, two fuels, one European standard diesel as reference (REF) and one pure biofuel like rapeseed methyl

ester (RME) have been used. Finally, in order to realize the same IMEP in the engine the injected amount of RME fuel was little bit increased due to its low heating value. In Table 2 the fuels characteristic are shown.

Table 1 Engine operating conditions

Nozzle type	**Fuel**	**SOI Pil**	**ET Pil**	**Dwell Time**	**SOI Main**	**ET Main**	**Pinj**
		[°]	**[μs]**	**[μs]**	**[°]**	**[μs]**	**[bar]**
A	**REF**	-15	274	1139	-4.5	532	620
B	**REF**	-14.5	276	1145	-4.3	531	620
C	**REF**	-14.2	271	1130	-4	526	620
A	**RME**	-15	274	1139	-4.5	552	620
B	**RME**	-14	277	1145	-3.8	550	620
C	**RME**	-14.5	271	1130	-4.3	573	620

Table 2 Fuels characteristic

Feature	**Method**	**REF**	**RME**
Density @ 15 °C [kg/m^3]	EN ISO 12185	833.1	883.1
Viscosity @ 40 °C [mm^2/s]	EN ISO 3104	3.141	4.431
Oxydation Thermal Stability @ 110°C [h]	EN 14112	-	6.5
Oxydation stability [mg/100ml]	EN ISO 12205		0.6
Lubricity @ 60 °C [μm]	EN ISO 12156-01	-	179
Cetane Number	EN ISO 5165	51.8	52.6
Low Heating Value [MJ/kg]	ASTM D4868	42.965	37.570
A/F st		14.54	12.44
C.F.P.P. [°C]	EN 116	-	-14
POV [meq O2/kg]	NGD Fa 4		16.60
TAN [mg KOH/g]	EN 14104		0.13
Carbon [%, m/m]	ASTM D 5291	85.22	77.11
Hydrogen [%, m/m]	ASTM D 5291	13.03	11.60
Nitrogen [%, m/m]	ASTM D 5291	0.04	0.03
Oxygen [%, m/m]	ASTM D 5291	1.45	11.25

Results and Discussion

A complete excursus of the spatial and temporal evolution of the sprays in the optically engine was performed for all the conditions of Table 1. Images of the jets at different time from the start of injection and with a statistically valid number of repetitions per each condition were recorded.

In Figure 2, some images of main injection for the three tested nozzles and for REF are reported. Images are in single-shot and have been recorded at 1500 rpm, with a low cycle variation (around 3-5 %). For a fixed crank angle after the start of main injection (ASOI), images have been reported in order to appreciate the differences between the investigated nozzles. The start of visible injection occurs at about 3° crank angles (about 0.3 ms) after the start of the drive current to the injector and this delay is due to electrical effects and the inertia of the needle. In Figure 2, the eight jets can be clearly distinguished. The injection has duration around 5° crank angles; no impingement phenomena can be detected except for the B nozzle at 4° ASOI even if the injection is ending. The jets move regularly in the bowl and have sufficient time to mix with air before the main autoignition. During the main injection evolution, some luminous spots in the combustion chamber due to the combustion of the pilot injection can be noted. For A and C nozzles, moreover, greater luminous emissions has been detected than B one. Even if these flames are not the SOC of main injection, the temperature and pressure is changing in the bowl. This affects the jets penetration. Finally, at 5° ASOI, different behavior in the last phase of the injection for the three nozzles is observed. In particular, the penetration is reducing for all the nozzles due to the end of injection, but the biggest quantity of fuel that scatters light have been detected for the C nozzle. This could be due to the smallest nozzle diameter that spreads the fuel in the bowl with a narrow dispersion angle.

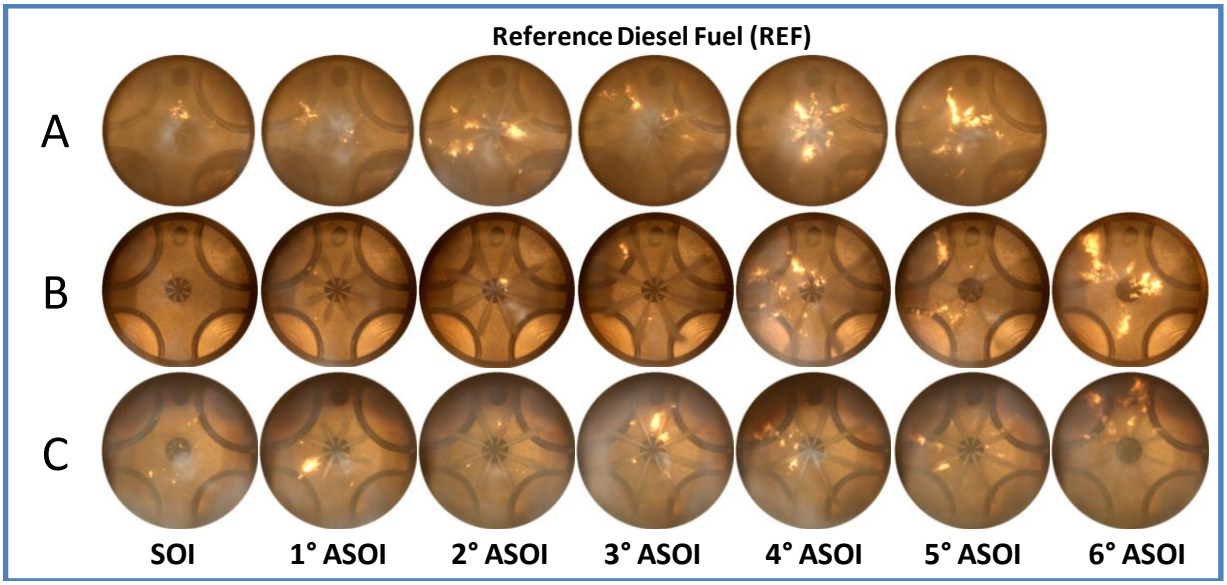

Figure 2 Different distributions of REF fuel at several degrees after the start of injection (ASOI) for the three injectors

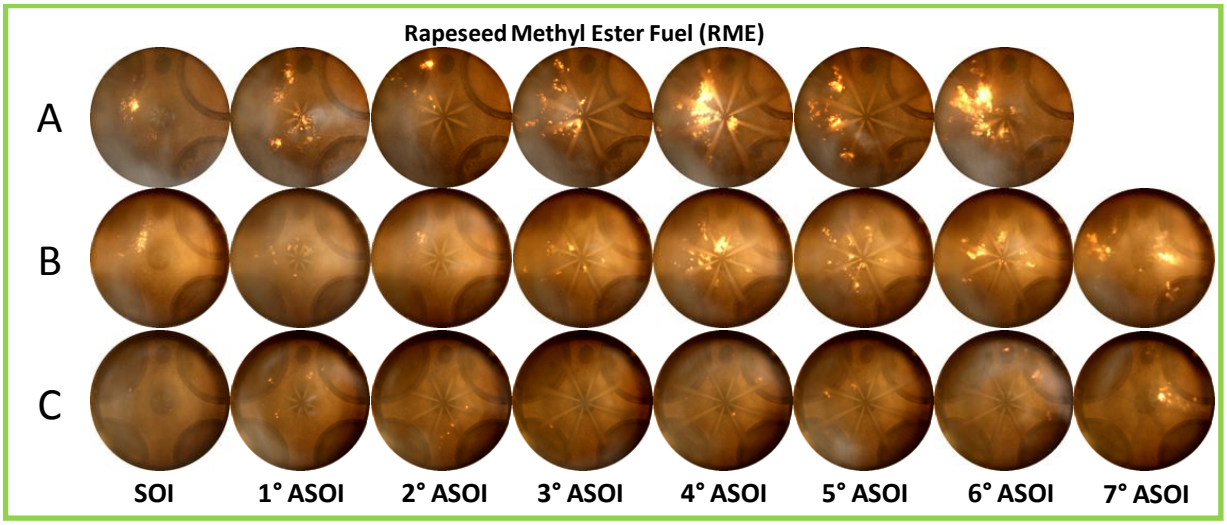

Figure 3 Different distributions of RME fuel at several degrees after the start of injection (ASOI) for the three injectors.

In Figure 3, the images of jets penetrations for the three nozzles and for RME fuel are reported. Regarding the jets evolution and distribution no evident differences was noted with respect to the previous cases. Longer injection period was analysed, because, as reported in table 2, longer energizing time was set in the ECU in order to realize the same IMEP of REF fuel. The main difference regards the development of visible flames into the bowl just at the start of the injection for all the nozzles. This is probably due to the higher cetane number of the fuel.

In Figure 4 the average spray tip penetration curves versus time for the three nozzles and two fuels tested are reported. The eight jets are analyzed and their lengths are measured from images of Figures 2 and 3. Five image repetitions at the same condition were performed to reduce the uncertainty due to the engine cycle variation. A SMR of 7% on the liquid length was evaluated for all the measured penetrations. Even if there is no sufficient time to stabilize the jets during the pilot injection, their tip penetrations were reported on the first row of the Figure 4 for both fuels. They evolve differently in the combustion chamber and affect greatly the following main injection because they ignite. Finally, it can be noted that the jets do not impinge the bowl wall.

Generally, the flow inside the injector is controlled by dynamic factors (injection pressure, needle lift, etc.) and geometrical factors (orifice conicity, hydrogrinding, etc.). For this reasons, the nozzle with larger hole diameter produces sprays with longer spray tip penetration than the nozzles with smaller holes. In Figure 4, second line, B and C nozzles for REF fuel showed longer penetrations than A one. In fact, A had the best combustion

efficiency of pilot injection that brings to higher temperature and pressure in the bowl than the other two cases. On the other hand, opposite trend was noted for RME. In this case B and C nozzle showed longer tip penetration than A one. This is due to the higher fuel density of RME.

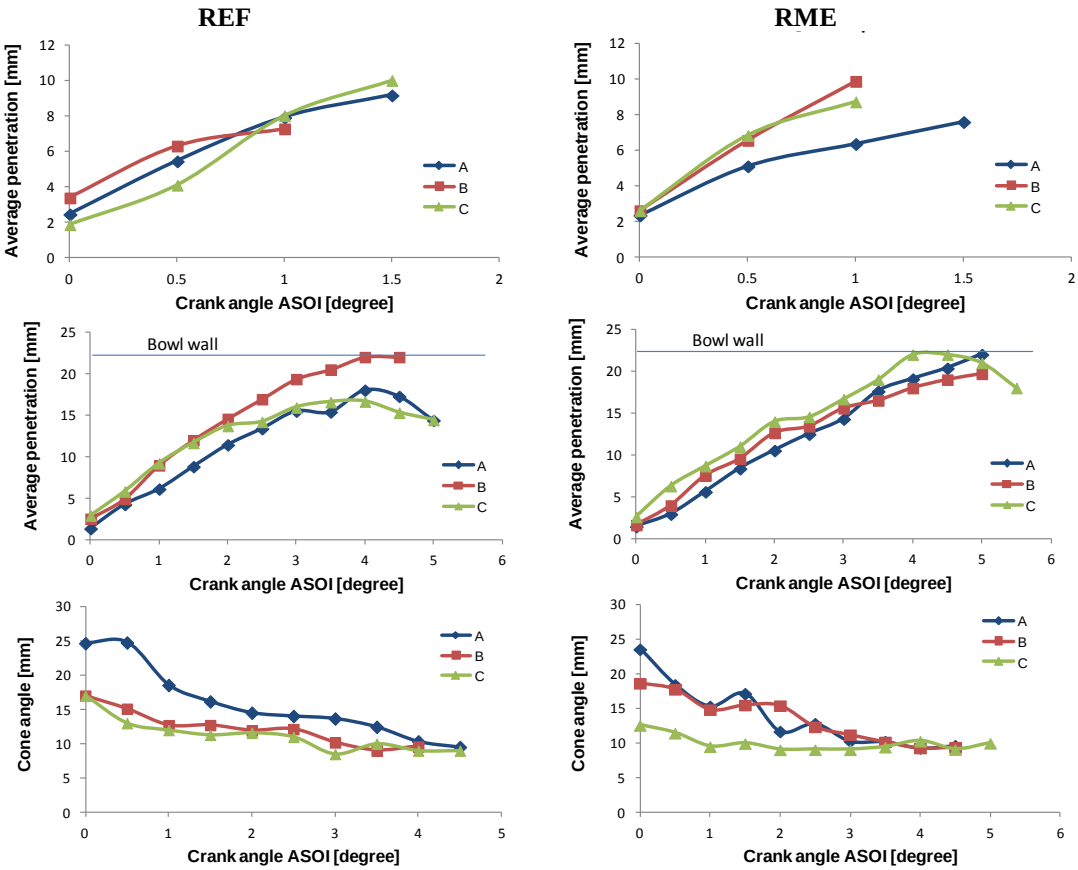

Figure 4 Effect of nozzle diameters on the pilot tip penetration (1st line), main tip penetration (2nd line) and dispersion angle (3rd line) for REF (left) and RME (right) fuels, respectively.

Another consideration is that the smallest nozzle diameters impress a higher initial velocity to the fuel resulting in a longer tip penetration, at equal injection pressure and at similar in-cylinder gas density. After 3° ASOI the average spray penetration curves change its slope and the impingement effects of liquid was noted only for the B nozzle when engine run with REF fuel. Probably, a good atomization has been realized for the fuel injected with the A and C nozzles. Two different reasons could justify this circumstance. For nozzle A the high temperature, and then mixture density, in the bowl and near the bowl wall could be responsible of good fuel evaporation. On the other hand, for nozzle C that has the smallest hole diameter, the good atomization produced smaller fuel droplets. These are more easily transported in the bowl, more easily evaporated, and, finally, mixed with the charge in the spray tip location. On the contrary, the impingent was clearly observed for all the nozzles injecting RME. In this case the high density and viscosity of the fuel produced longer tip penetrations than the REF case; however, the evaporation process increases because RME has higher cetane number than REF. This favored the mixing of the RME fuel with air into the bowl. Finally, on third line of Figure 4, the dispersion angles are reported. They are in line with the geometrical parameters that characterize the several nozzles. In particular, the nozzle with larger hole diameter produces fuel droplets with larger diameter than the nozzles with smaller holes. After 2° ASOI, the dispersion angle of A, B and C, nozzles injecting REF fuel settle around 14°, 12° and 11°, respectively. But at the end of the injection they shift to the same value around 10°. For RME, smaller dispersion angles were measured for A and C nozzles. After, 2° ASOI they are 12.5°, 15°, and 10° for A, B and C nozzle, respectively. Finally, they reach the same value at the end of the injection around 10°. This is due to the high in-cylinder temperature and pressure that improve the evaporation process.

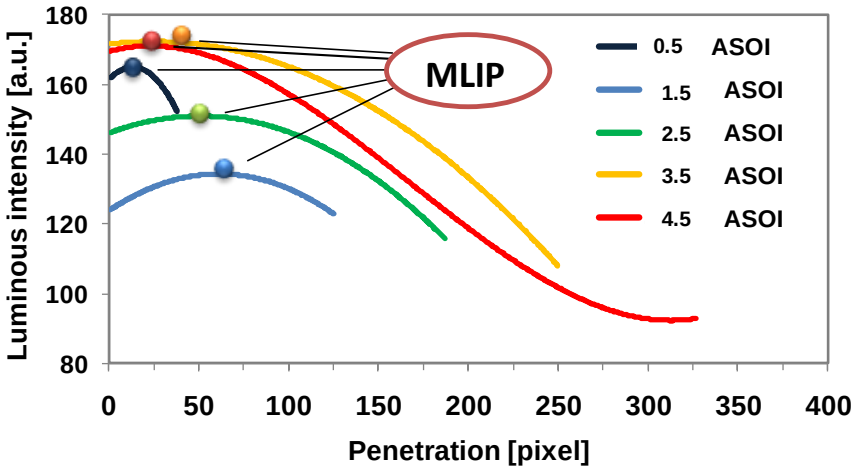

Figure 5 Luminous intensity along the jet axis for A nozzle and REF fuel.

When the fuel is injected into the combustion chamber, it is slowed down and spread out by the in-cylinder gas, the temperature of the jet increases and local inter-phase transport phenomena occur. These series of processes characterises the jet structure, a dense core and a less dense boundary are distinguishable. Using image processing techniques, the density of the jet has been investigated coupling the density to the image luminosity [4]. In Figure 5 the luminous intensity along the jet axis has been traced for several crank angles, for the REF. Firstly, for a fixed crank angle, it can be observed that the lowest density values corresponds to the spray tip, where the fuel had more time to mix with the air and the vaporization process is occurring. The peaks of luminosity are visible in the centre or in the first part of the curves, due to the dense core of the jet that hasn't yet been in contact with the in-cylinder gases; this last observation involves a more accurate investigation. In particular, in the early injection it has been noticed that the Maximum Luminous Intensity Point (MLIP) is placed around the centre of the jet, then its position draws back and settles closer to the nozzle.

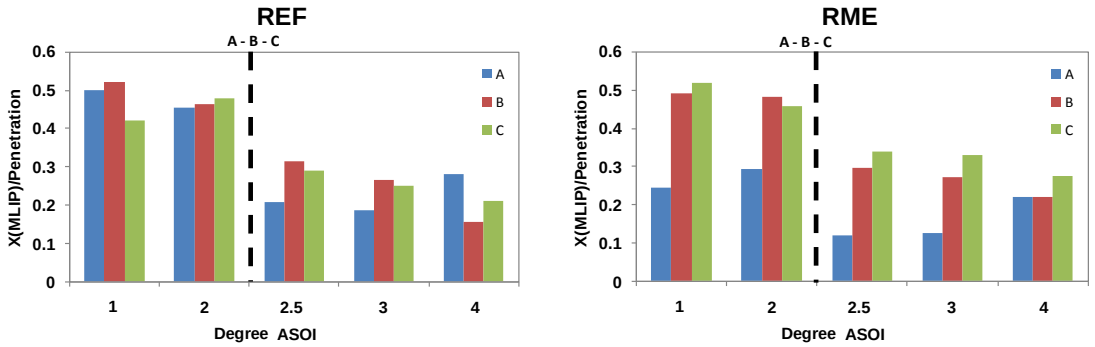

Figure 6 Normalized maximum luminous intensity point versus degree after start of main injection

Figure 6 shows the MLIP position normalized with respect to the instantaneous main penetration for both fuels and the three nozzles investigated, two phases can be distinguished in each graph. The first corresponds to the early injection, and the histograms have values around the 0.5, except nozzle A of RME fuel that has value around 0.25; whilst in the second phase the values decrease suddenly, and reach about the 0.25-0.30 mark. RME decreases up to 0.12. At the beginning, the fuel injected in the combustion chamber is surrounded by bubbles because of the cavitation effects inside the injector nozzle, and then during the penetration of the jet, they collapse because of the surface tension and the aerodynamic forces producing oscillations on the jet surface. As the fuel spray penetrates in the combustion chamber its periphery starts atomizing, thereby creating small droplets and reducing the volume of the jet core. During this last phase, the effect that influences the spray behaviour changes, at beginning the jet can be considered completely liquid, after it consists of a dense core and a vaporizing periphery made up of small droplets. According to this analysis, in the first phase the centre of mass of the jet is placed in the geometric centre of the jet shape; in the second phase, after the atomization, it moves toward the nozzle because the farthest part of the spray has less mass than the nearest one, it is vaporizing. In this case, the centre of mass is linked to the denser portion of the jet, it is characterized by higher light reflection and the positions that the MLIP assumes during the jet penetration permit to identify the dominant factor on the jet behaviour and individuate the point of transition from one to another. Results obtained from this image-based method have

been compared with transition time of Naber and Siebers [5] and with the break up time of Hiroyasu and Arai [6] and it gives very interesting results [4]. In that paper, we concluded that the point of separation between the fuel injected dominant phase and gas entrainment dominant phase can be experimentally determined by Figure 6. In particular, for all nozzles investigated and for both the fuels tested the break up occurred between 2°-2.5° ASOI.

Summary and Conclusions

An experimental investigation of the nozzle flow number impact on diesel and RME spray evolutions has been performed carrying out the investigations in optical single-cylinder engine. Three injector configurations for Euro 5 diesel engines, with 136, 122 and 107 μm hole nozzle diameters have been investigated into the cylinder for injection strategy consisted of two injections per cycle.

The analysis of the jets showed a regular and uniform development for all the nozzles and fuels investigated except at early time from the start of injection. Concerning the main tip penetration, no linear trend has been noted with the reduction of nozzle flow number. However, favourable effects due to the combustion of pilot injection that improve the evaporation and, then, the mixture process in the bowl have been observed. Moreover, at fixed crank angle after the start of injection, longer spray tip penetrations of RME fuel was detected due to its higher density. Analysing the dispersion angle, they were also affected by the in-cylinder temperature and pressure and they were smaller than REF fuel for A and C nozzles.

The luminous intensity analysis of images has been correlated with the density distribution of the liquid phase of the spray. It has revealed that the spray tip has lower density values, while higher values are evident in the centre or in the first part of the curves. Finally, the break up time was measured by means of experimental analysis of the luminous intensity and it occurred between 2°-2.5° ASOI for all nozzles and both fuels investigated.

Definitions/Abbreviations

ASOI: After Start Of Injection
BMEP: Brake Mean Effective Pressure
CCD: Charge Coupled Device
CR: Common Rail
CW: Continuous Wavelength
DI: Direct Injection
ECU: Electronic Control Unit
EGR: Exhaust Gas Recirculation
IMEP: Indicated Mean Effective Pressure
MLIP: Maximum Luminous Intensity Point
REF: Reference Diesel Fuel
RME: Rapeseed Methyl Ester
TDC: Top Dead Center
VSA: Variable Swirl Actuator

Acknowledgements

The authors wish to thank Mr. Carlo Rossi and Bruno Sgammato for maintaining the experimental apparatus and for their precious help.

References

[1] Payri, R., Salvador, F. J., Gimeno, J., Zapata, L. D., *Fuel* 87: 1165-1176 (2008)
[2] Payri, R., Salvador, F. J., Gimeno, J., de la Morena J., *Applied Thermal Engineering*, 29: 2051-2060 (2009)
[3] Heywood, J. B., *Internal Combustion Engine Fundamentals*. Mc Graw-Hill, NewYork (1988)
[4] Mancaruso, E., Sequino, L., Vaglieco, B. M., Fuel 90: 2870-2883 (2011)
[5] Naber, J. D., Siebers D. L., SAE paper no. 960034; (1996)
[6] Hiroyasu, H. and Arai, M., Trans. JSME, 44, 3208-3220(1980)